

# Aromatic components of two ferric enterobactin binding sites in *Escherichia coli* FepA

Zhenghua Cao, Zengbiao Qi, Cathy Sprencel, Salete M. C. Newton and Phillip E. Klebba\*

Department of Chemistry and Biochemistry,  
University of Oklahoma, Norman, OK 73019, USA.

## Summary

Ferric enterobactin is a catechololate siderophore that binds with high affinity ( $K_d \approx 10^{-10}$  M) to the *Escherichia coli* outer membrane protein FepA. We studied the involvement of aromatic amino acids in its uptake by determining the binding affinities, kinetics and transport properties of site-directed mutants. We replaced seven aromatic residues (Y260, Y272, Y285, Y289, W297, Y309 and F329) in the central part of FepA primary structure with alanine, individually and in double combinations, and determined the ability of the mutant proteins to interact with ferric enterobactin and the protein toxins colicins B and D. All the constructs showed normal expression and localization. Among single mutants, Y260A and F329A were most detrimental, reducing the affinity between FepA and ferric enterobactin 100- and 10-fold respectively. Double substitutions involving Y260, Y272 and F329 impaired (100- to 2500-fold) adsorption of the iron chelate more strongly. For Y260A and Y272A, the drop in adsorption affinity caused commensurate decreases in transport efficiency, suggesting that the target residues primarily act in ligand binding. F329A, like R316A, showed greater impairment of transport than binding, intimating mechanistic involvement during ligand internalization. Furthermore, immunochemical studies localized F329 in the FepA ligand binding site. The mutagenesis results suggested the existence of dual ligand binding sites in the FepA vestibule, and measurements of the rate of ferric enterobactin adsorption to fluoresceinated FepA mutant proteins confirmed this conclusion. The initial, outermost site contains aromatic residues and probably functions through hydrophobic interactions, whereas the secondary site exists deeper in the vestibule, contains both charged and aromatic residues and probably acts through hydrophobic and electrostatic bonds.

## Introduction

Gram-negative bacteria acquire iron with transport systems that usually involve the elaboration of siderophores and the uptake of their ferric complexes. For example, enterobactin, the native siderophore of *Escherichia coli*, forms a hexaco-ordinate complex with  $Fe^{3+}$ , which enters prokaryotic cells through a multicomponent cell envelope transport system. An outer membrane (OM) ligand-gated porin (LGP), FepA, initiates ferric enterobactin (FeEnt) uptake into the cell; the periplasmic-binding protein (FepB) and an inner membrane complex of proteins (FepCDG) finish the transport process into the cytoplasm.

Multiple functional domains exist within ferric siderophore receptors such as FepA. Besides an external ligand binding site, they contain a transmembrane channel (Rutz *et al.*, 1992; Liu *et al.*, 1993) and a globular N-terminal domain that lodges within the pore (Buchanan *et al.*, 1999). FepA is ligand gated (Rutz *et al.*, 1992; Killmann *et al.*, 1993), in that the binding of FeEnt on its exterior triggers a series of events that ultimately open the pore, resulting in internalization (Jiang *et al.*, 1997). The N-terminal domain was proposed to regulate this transport reaction (Buchanan *et al.*, 1999); the fact that it physically blocks the channel requires that it undergoes structural rearrangements during ligand uptake.

The chemistry of FeEnt may explain its interaction with proteins. The catechololate iron complex carries a net charge of  $-3$ , portending the involvement of aromatic and basic residues in its recognition by FepA. Mutagenesis verified the importance of basic residues (R286, R316) in FeEnt binding (Newton *et al.*, 1997) and, in this report, we consider the function of aromatic amino acids in adsorption. FepA and another siderophore receptor, FhuA, contain aromatic residues in their surface loops that encircle the external entrances to their underlying pores (Fig. 1). These amino acids may function in the recognition and discrimination of the many ferric siderophores of the microbial world, or they may create a non-specific, non-polar surface that absorbs these hydrophobic molecules from the environment. We used site-directed mutagenesis and fluorescence spectroscopy to study the participation of aromatic amino acids in the recognition of FeEnt by FepA. Among seven conserved aromatic residues that we substituted with alanine, changes at three, Y260, Y272 and F329, affected the affinity of the FeEnt–FepA interaction. These residues define two sites, one on the

Accepted 5 July, 2000. \*For correspondence. E-mail peklebba@ou.edu; Tel. (+1) 405 325 4969; Fax (+1) 405 325 6111.

surface of the vestibule and another deep within it. The identification of these separate binding domains, and measurements of the rate of FeEnt binding to FepA mutants with alterations in them, support the two-stage model of siderophore binding to TonB-dependent OM receptor proteins (Payne *et al.*, 1997).

## Results

### Target residues for mutagenesis

Several previous experiments suggested that the central portion of FepA contains residues that interact with ligands (Murphy *et al.*, 1990; Rutz *et al.*, 1992; Newton *et al.*, 1997). Within this region of the *Escherichia coli* receptor, we identified numerous residues that we considered potentially important in FeEnt uptake, because they are mostly conserved in the FeEnt transport proteins of Gram-negative bacteria, but not in the other LGP of *E. coli*. The comparison (Fig. 1) highlighted seven aromatic residues, including five tyrosines (260, 272, 285, 289 and 309), one tryptophan (297) and one phenylalanine (329). Among these, Y260 was distinct, in that it was also conserved in BtuB, FhuA and FhuE.

The multideterminant nature of a ligand–receptor interaction may prevent single substitutions, even for amino acids involved in binding, from producing significant phenotypical effects (Newton *et al.*, 1997). However, double mutagenesis, the pairwise alteration of candidate residues, yields more recognizable defects that may identify mechanistically relevant amino acids. Our initial approach to evaluating aromaticity in FeEnt recognition involved single and double Ala substitutions for the seven aromatic residues of interest, yielding 28 site-directed mutants. The results focused attention on three mutants (Y260A, Y272A and F329A), which we combined with another mutation (R316A) previously found to be critical to the binding reaction (Newton *et al.*, 1997), yielding three more mutants. In addition, we made single and double Ala substitutions for five negatively charged amino acids in the same general region of *E. coli* FepA, yielding 15 more mutants. Finally, we combined two double mutants with the chemically modifiable mutation E280C to facilitate their biophysical analysis. In total, we engineered and analysed about 50 mutant FepA proteins.

The substitution mutations did not affect the expression of FepA: Western blots showed all the mutant proteins at wild-type levels. The immunoblots also revealed that residue F329, which exists in L4, in a region of FepA structure that was not resolved by the crystallographic analysis, is a structural determinant of the dominant surface epitope (Murphy *et al.*, 1990; Rutz *et al.*, 1992; Kuhn *et al.*, 1998) recognized by anti-FepA monoclonal antibody (mAb) 45. Any FepA protein containing F329A was not recognized by mAb 45 in immunoblots (Fig. 2) or

flow cytometry (data not shown). This antibody blocks the binding of FeEnt and colicins B and D (Murphy *et al.*, 1990), and FeEnt binding to FepA inhibits recognition by mAb 45 (Cao, 1999). None of the other mutations that we engineered affected the recognition of FepA by mAb 45, including E319A, five residues upstream of F329. These immunochemical data therefore localize F329 on a well-exposed external surface of L4, which is in intimate proximity to, or a component of, a FeEnt binding site.

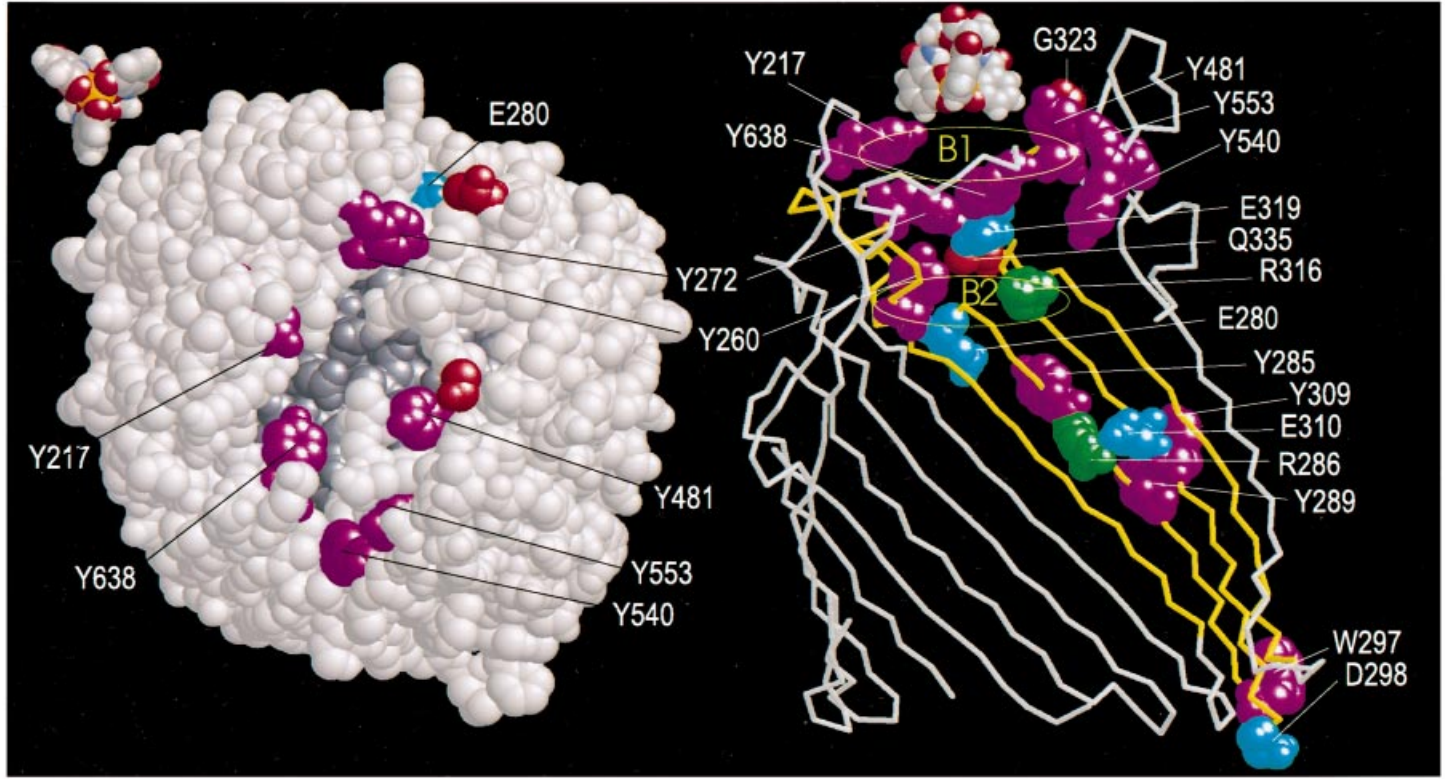
### Affinity screening

The nature of binding and transport assays that involve triplicate measurements of FeEnt adsorption/uptake at 12 concentrations (Newton *et al.*, 1999) made thorough analysis of so many constructs problematical. Therefore, and because we anticipated only a percentage of the total mutations to affect ligand–receptor interactions (< 20%; Newton *et al.*, 1997, this study), we sought methods of rapidly distinguishing constructs with aberrant phenotypes from those that function at wild-type levels. The use of affinity screening was one step towards this end. The ratio of <sup>59</sup>FeEnt binding or transport at the wild-type  $K_d$  (or  $K_m$ ) and at a much higher concentration (e.g.  $1000K_d$  or  $1000K_m$ ) identified impaired FepA proteins (Fig. 3) for subsequent thermodynamic and kinetic analysis. This approach singled out Y260, Y272 and F329. The substitution Y260A strongly decreased affinity for FeEnt, whereas the effect of F329A was most apparent and that of Y272A was only seen in double combinations (Fig. 3). Double substitutions joining Y260A, Y272A or F329A with R316A confirmed the importance of the aromatics in FeEnt binding: each of the double mutants showed much lower affinity than R316A alone. Alanine substitutions for all the other residues that we tested had no significant effects on FeEnt adsorption.

### Binding equilibria

Recent methodological improvements (Newton *et al.*, 1999) enhanced the sensitivity of <sup>59</sup>FeEnt binding and uptake tests, which enabled us to accurately assess the impact of the site-directed mutations on the receptor protein. Among all the single aromatic mutants observed by affinity screening, and also including R316A, only Y260A showed an obvious (about 100-fold) reduction in adsorption affinity (Fig. 4): the  $K_d$  of the FeEnt–FepA binding reaction increased from the wild-type level of 0.1 nM to 10 nM. Y272A did not change affinity at all, whereas F329A and R316A created only nominal alterations in  $K_d$ , to 0.2 nM and 0.4 nM respectively. Double combinations of these three mutations created predictable

A



B

	Y260	Y272	E280	R286	D298	E310	R316	E319	E326	F329					
	S5	L3	S6	S6	S6	S7	S7	L4	L4	S8					
N	MKDQHRGIRT	VREEFAV	SEK	NSRIT	IKR	QAPSYR	ETTQSNNTLA	YTGKDLGF	VEKLDANAYV	LEKKR	YSADDDKNGYAG	NVKGPNH	TRIATRSMNFNFD		
B	NTVDLDMGFS	RQGNL	FAGDTMNNANS	DFSD	SLYGKETNAMYR	ENYALTHRGV	YDWG	TSRASVGYDY	TRNAR	QREGLAGGPEGA	PT	AG	GYDTARKL	NWRAAAEASVPPFH	
P	QTLFEAGFS	RQGNL	YAGDTQNTNSNNYVK	QMLGHE	TNRMYR	ETYSVTHRGE	WDFG	SSLAYLQYEH	TRNSR	INEGLAGGTEGI	FDPNNAG	FY	TATLR	DLTAHGEVNLPLH	
S	QILDFEAGYS	RQGNL	YAGDTQNSNSNAVTK	SLAQSGRE	TNRLYR	QNYGLTHNGI	WGWG	QSRLGFYEH	TDNTR	MNEGLSGGGEGR	ITNDQFTTNRLT	SYRTS	GEVNV	VPVI	
S	QSLELEAGYS	RQGNL	YAGDTQNTNTNQLVK	DNYGKETNRLYR	QNYSLTWNGG	WNNGV	TTSNWWQYEH	TRNSR	MPEGLPGGTEGI	FDP	KASQKYADADLN	DVTLH	SEVSL	PFD	
E	QSLELEAGYS	RQGNL	YAGDTQNTNSDSYTR	SKYGDE	TNRLYR	QNYALTWNGG	WNGV	TTSNWWQYEH	TRNSR	IPEGLAGGTEGK	FNE	KATQDFVDIDL	DVMLH	SEVNL	EPID
C	QNHDFTAGYG	FDRQD	DSDSLDK	DSDSLDK	NRLER	QNYSVSHNGR	WDYG	TSELKYYGK	VENK	NPGNS	PITSE	SNIVD	GKTYL	PLPT	
F	QYYDGEADMP	GGLSRA	DYD	ADR	WQSTRPYDR	FWGRRKLASL	GYQFPDS	QHKFNIQGFY	TQTLRSGYL	EQGK	RITLSP	RNYV	VRGIE	PRYS	
B	WSGFVRGYG	DNRTN	Y	DAY	YSPGSPLLDTR	KLYSQSDWAG	LRYN	GELIKSQLIT	SYSH	SKDYN	DPHYGRYD	SSATL	DEM	QYTV	WANNVIVG
I	QTGLQYSDRL	DIMGTG	TLNIDESR	QLQLITQYK	YK	YK	YK	YK	YK	YK	YK	YK	YK	YK	
A	TNFTFLSYFQ	NEPETGY	YGWLPKEG	TVEPLP	NGKRLPTDF	NEGA	KNNYYSR	NEKMGVGS	YK	YK	YK	YK	YK	YK	
E	LSAGYEYQRI	DVNSPTWGG	LPRWNTD	GSSNSYDR	ARSTAPD	WAYNDKE	INR	VFMTLKQQA	DTWQA	TLNATHSEVE	FDSKMMYV	DAYV	VNKAD	GLMVP	YSNY

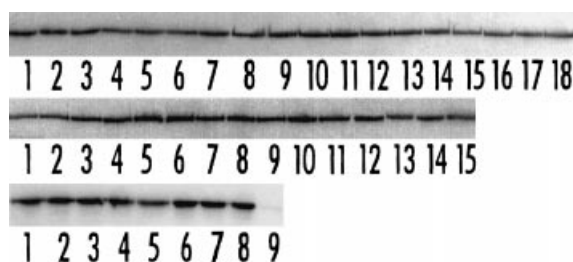


**Fig. 2.** Expression of FepA mutant proteins. KDF541 carrying *fepA* or its mutant derivatives, which were grown in MOPS minimal media for binding and transport studies, was lysed in sample buffer and subjected to SDS-PAGE and Western immunoblotting with anti-FepA mAbs and [<sup>125</sup>I]-protein A. Top. Lane 1, + + 2, (Ala substitution at) Y260; 3, Y272; 4, Y285; 5, Y289; 6, W297; 7, Y309; 8, F329; 9, Y260/Y272; 10, Y260/Y285; 11, Y260/Y289; 12, Y260/W297; 13, Y260/Y309; 14, Y260/F329; 15, Y272/Y285; 16, Y272/Y289; 17, Y272/W297; 18, Y272/Y309. Middle. Lane 1, Y272/F329; 2, Y285/Y289; 3, Y285/W297; 4, Y285/W309; 5, Y285/F329; 6, Y289/W297; 7, Y289/Y309; 8, Y289/F329; 9, W297/Y309; 10, W297/F329; 11, Y309/F329; 12, R316; 13, Y260/R316; 14, Y272/R316; 15, R316/F329. Bottom. Western immunoblot with anti-FepA mAb 45 and [<sup>125</sup>I]-protein A. Lanes 1–7 contain the same samples as in the top blot; lane 8, R316A; lane 9, F329A. Note the feeble reactivity of this antibody with F329A in lane 9.

and roughly additive reductions in affinity, from 100- to 2500-fold, which confirmed the relative order of importance seen in the comparisons of single mutants: Y260 > R316 > F329 > Y272 (Table 1). As their affinity decreased, the double mutants manifested a corresponding decrease in FeEnt binding capacity (Table 1, Fig. 4). This reduction probably derived from the inability of the experiment to accurately measure the capacity of low-affinity binding reactions, because of the rapid dissociation of the ferric siderophore from such defective receptors, relative to the time required for the <sup>59</sup>FeEnt binding determination. Finally, FeEnt adsorbed more slowly to Y260A and its combinations than to the wild-type receptor protein or other mutants not including Y260A. *In vivo*, binding to FepA reached equilibrium in less than 5 s at 0°C, whereas for Y260A in the same conditions, even a 1 min incubation was insufficient to reach equilibrium (data not shown).

### Binding kinetics

The effects of mutagenesis suggested the existence of dual binding sites for FeEnt in the vestibule of FepA: an exteriormost location populated by aromatic residues, including Y272 and F329, and an internal site with both charged and aromatic amino acids, including Y260 and R316 (Fig. 1). The FeEnt adsorption reaction occurs in two distinct stages (Payne *et al.*, 1997), and it was of interest to study the rates of siderophore binding to the mutants with lower affinity. To do so, we combined the covalently modifiable mutation E280C with the double mutants Y272A/F329A and Y260A/R316A. E280 exists in L3 on the external surface of FepA, removed from the mouth of the vestibule (Fig. 1); its substitution with Cys and subsequent reaction with either fluorescent or paramagnetic (Jiang *et al.*, 1997) labels does not affect FeEnt binding and transport. We purified the two triple mutant proteins, modified them with fluorescein and spectroscopically characterized their FeEnt adsorption rates. The mutants showed distinctly different kinetics from wild-type FepA and from each other (Fig. 5; Table 2). Although both mutant proteins bound the siderophore, neither underwent the complete association reaction of wild-type FepA, as shown by the lower amplitude of fluorescence quenching engendered by FeEnt binding to them. The Y260A/R316A mutation dramatically curtailed the second stage of the adsorption reaction, without impairment of the initial phase. Conversely, Y272A/F329A decreased the amplitude of both binding phases. These results strongly support the hypothesis of an initial binding site affected by the mutation Y272A/F329A and a second, subsequent site influenced by Y260A/R316A (see *Discussion*). Neither double mutation significantly changed the rate of initial adsorption ( $k_1$  in Table 2), as expected for a process that is presumably diffusion limited. However, the high concentration of FeEnt (10 μM) required for saturation of the mutants accelerated the association reaction so much that we could not measure precisely the first binding phase. Both double mutations increased the velocity of the second phase ( $k_3$  in Table 2), but the final determination

**Fig. 1.** Top. Aromatic amino acids encircling vestibule openings of FepA (left) and location of mutagenesis targets in FepA (right). FeEnt (top left) enters the bacterial cell through the FepA protein. In the space-filling model of FepA (Buchanan *et al.*, 1999), aromatic residues are coloured magenta, and the residues of the N-terminal plug domain are dark grey. Residues G323 and Q335 are coloured red. They are the nearest crystallographically solved residues in L4 to F329, which was not described (Buchanan *et al.*, 1999), and hence is not shown. The backbone representation on the right shows the mutagenesis targets in space-filling form and other residues proposed to constitute the B1 binding site. The backbone in the region of mutagenesis, between residues 247 and 335, is yellow. The N-terminal domain and portions of the β-barrel do not appear in this representation. Bottom. Sequence alignment of FeEnt transporters and *E. coli* LGP. The top six proteins [*Neisseria gonorrhoeae* FetA (N), *Bordetella pertussis* BfeA (B), *Pseudomonas aeruginosa* PfeA (P), *Salmonella typhimurium* FepA (T) and IroN (S), and *E. coli* FepA (E)] transport FeEnt. The seventh protein [*E. coli* Cir (C)] transports the degradation products of FeEnt, Fe-DHBS. The bottom six sequences are from other ligand-gated porins of *E. coli* [FecA (F), BtuB (B), IutA (I), FhuA (A), FhuE (E)]. The sequences were aligned by the PILEUP algorithm (GCG, Madison WI, USA) and manually adjusted on the basis of the FepA and FhuA crystal structures. β-Strands are overlined; residues in bold type are on the outside of the barrel. The strands of the FepA β-barrel in the region of interest are enumerated S5–S8; surface loops L3 and L4 are also shown.

of these rates awaits more accurate measurements by other methods.

### Transport

We performed siderophore nutrition tests as a first indicator of transport phenotype. In this assay, FepA mutants may show a variety of effects that differentiate them from wild type (Newton *et al.*, 1999). Constructs involving substitutions for Y260, Y272 or F329 produced three principal results, larger, fainter and fuzzy halos (Fig. 6, Table 1). These mutants, which showed transport deficiencies (see below), grew more slowly on plates than strains expressing wild-type FepA so, at any given time, their siderophore nutrition tests were fainter. Halos derived from wild-type strains developed in 6 h, whereas those from the mutant strains were sparse at that time and required as much as 24 h to reach a similar density. In

some cases (Fig. 6), the mutants produced two growth rings: one nearly the same size as the wild type; and a second larger ring.

Uptake screening (Fig. 3) again underscored the inadequacies of Y260A and F329A, but, in this assay, the two mutants were equally, and completely, impaired. None of the other single mutants were deficient in transport screening assays, nor were they defective when combined with each other and tested at a variety of other concentrations. Transport assays over a full range of concentrations clarified the effects of the single Ala substitutions on FeEnt uptake. The maximum velocity of transport was comparatively intransigent. Among the mutations that we generated, only R316A reproducibly decreased the transport rate, but its impact was minor. The  $V_{\max}$  of FeEnt uptake by FepAR316A ( $117 \text{ pmol} \cdot \text{min}^{-1} \cdot 10^{-9} \text{ cells}$ ) was 65% of the wild-type rate ( $181 \text{ pmol} \cdot \text{min}^{-1} \cdot 10^{-9} \text{ cells}$ ), and its combinations

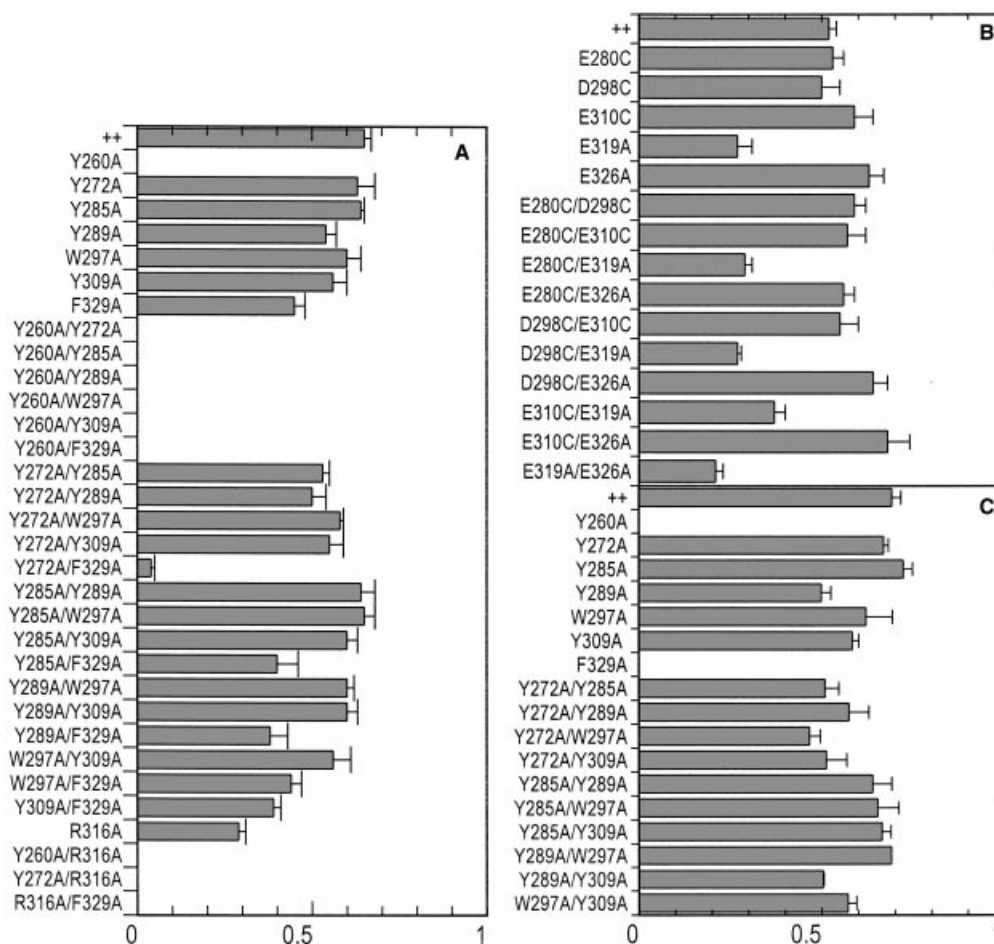


**Fig. 3.** Affinity screening of FepA mutants.

A.  $K_d$  screening of aromatic and basic substitution mutants.  $^{59}\text{FeEnt}$  binding assays were performed at 0.2 nM and 70 nM. The bars depict the ratio of FeEnt bound at these two concentrations. The error bars represent the standard deviations from three experiments.

B.  $K_d$  screening of acidic substitution mutants.  $^{59}\text{FeEnt}$  binding assays were performed at 0.2 nM and 70 nM.

C.  $K_m$  screening of aromatic substitution mutants. Ferric enterobactin uptake assays were performed at 0.3 nM and 100 nM. The bars depict the ratio of FeEnt transported at these two concentrations. The error bars represent the standard deviations from three experiments.

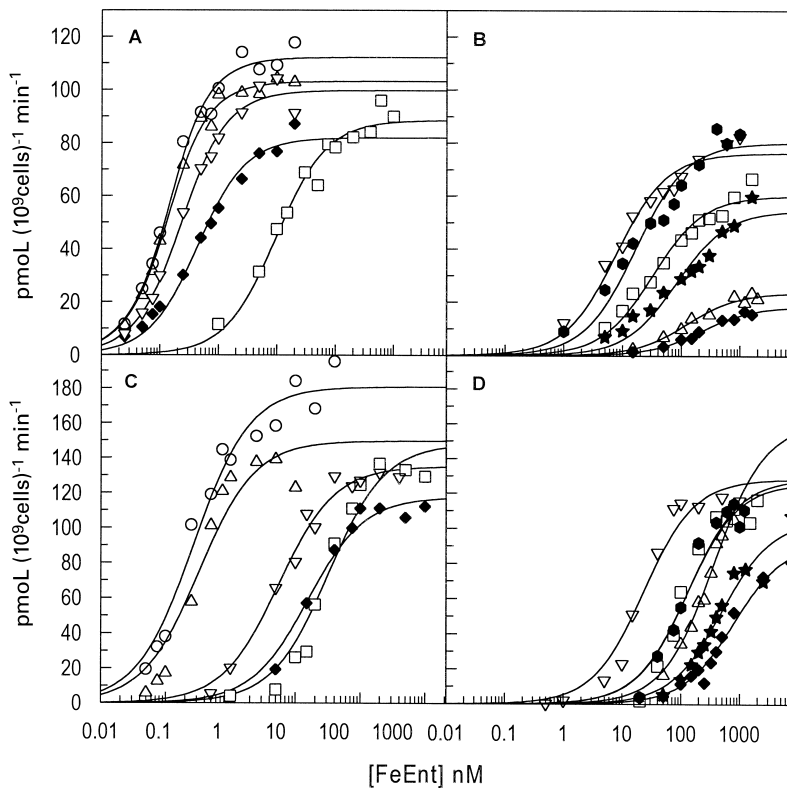


**Fig. 4.** Concentration dependence of FeEnt binding and transport by FepA mutant proteins. Top.  $^{59}\text{FeEnt}$  binding. KDF541 harbouring mutant *fepA* genes on pUC18 (pITS449) derivatives was analysed at 12 concentrations near  $K_d$ , with each data point collected in triplicate and averaged. The concentration of FeEnt was plotted logarithmically to demonstrate the large decreases in affinity that some of the mutations produced. The experiments were repeated at least three times and averaged to generate the plotted curves. Bottom.  $^{59}\text{FeEnt}$  uptake. The absolute rates of FeEnt transport were measured in the same strains. A and C. Wild-type FepA ( $\circ$ ); single mutants: Y260A ( $\square$ ), Y272A ( $\Delta$ ), R316A ( $\blacklozenge$ ) and F329 ( $\nabla$ ). B and D. Double mutants: Y260/Y272A ( $\square$ ), Y260/R316A ( $\blacklozenge$ ), Y260/F329A ( $\Delta$ ), Y272/R316A ( $\bullet$ ), Y272/F329A ( $\nabla$ ), R316/F329A ( $\star$ ).

showed similar decreases. Changes in  $K_m$ , however, revealed that the alanine substitutions did not always affect transport as they did binding (Table 1, Fig. 4). The relative importance of the four residues was again

Y260 > R316 > F329 > Y272, but Ala substitutions for R316 and F329 created disproportionate decreases in overall transport affinity, relative to their effects on binding (Table 1). In most cases, binding defects created

**Table 1.** Phenotypic properties of FepA aromatic/charge substitution mutants.

FepA mutant	Ferric enterobactin								
	Binding <sup>a</sup>			Transport <sup>b</sup>			Colicin B	Colicin D	
	Binding ratio	$K_d$	Capacity	$K_m$	$V_{max}$	Nutrition	Killing <sup>c</sup>	Killing <sup>c</sup>	
+	+	0.65	0.086	112	0.27	181	19	100	100
Y260A	0	9.7	88	33	148	23	50	100	
Y272A	0.63	0.085	103	0.33	150	19	100	100	
R316A	0.29	0.40	82	16	117	22	2.5	8	
E319A	0.27	0.59	136	9.2	184	22	100	100	
F329A	0.45	0.18	100	5.5	135	19	50	100	
Y260A/Y272A	0	33	60	128	126	25	50	100	
Y260A/R316A	0	222	18	793	93	23	2.5	8	
Y260A/F329A	0	126	24	367	161	25	50	100	
Y272A/R316A	0	17	80	133	129	24	2.5	8	
Y272A/F329A	0	7.8	76	23	128	23	50	100	
R316A/F329A	0	83	55	486	105	24	2.5	8	

**a.**  $K_d$  (nM) and capacity [ $\text{pmol bound (}10^9 \text{ cells)}^{-1}$ ] were determined from the concentration dependence of FeEnt binding by analysing the mean values from three independent experiments with GRAFIT 4 (Erithacus), using the 'bound versus total' equation. The mean standard errors for  $K_d$  and capacity were 14% and 3% respectively.

**b.**  $K_m$  (nM) and  $V_{max}$  [ $\text{pmol min}^{-1} (10^9 \text{ cells)}^{-1}$ ] of uptake were determined from the concentration dependence of FeEnt transport by analysing the mean values from three independent experiments with GRAFIT 4 (Erithacus), using the 'enzyme kinetics' equation. The mean standard errors for  $K_m$  and  $V_{max}$  were 19% and 5% respectively. Nutrition test results for FeEnt present the diameters of growth halos in millimetres.

**c.** Colicin killing was determined by measuring the susceptibility of KDF541 expressing the mutant FepA proteins to limiting dilutions of colicins B and D, and is expressed as a percentage of the killing observed for KDF541/pITS449 (*fepA*<sup>+</sup>).

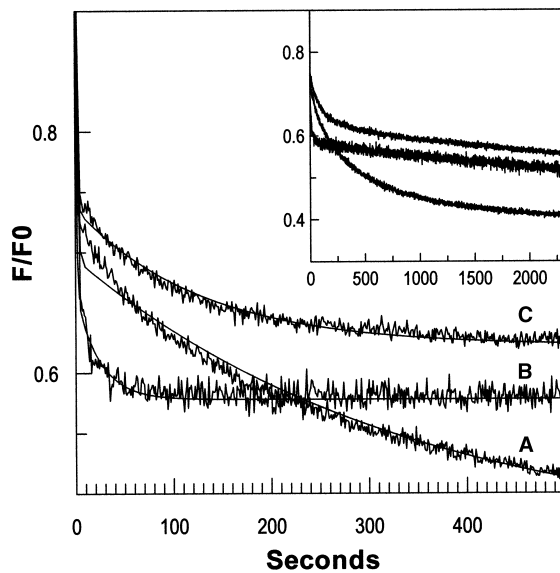


**Fig. 5.** Time course of FeEnt binding to mutant FepA proteins. The FepA mutant proteins E280C (A), Y260A–E280C–R316A (B) and Y272A–E280C–F329A (C) were purified (Payne *et al.*, 1997), labelled with IAF and diluted to a final concentration of 25 nM in 50 mM MOPS, pH 7, containing 1 mM dodecyl maltoside and 60 mM NaCl. The samples were equilibrated at 25°C for 1 h before the addition of FeEnt (10  $\mu$ M in the same buffer). The time course of binding was performed with excitation and emission wavelengths set at 490 nm and 520 nm respectively. The inset displays the raw data. For the determination of kinetic constants (Table 2), the gradual linear decay of the curves (after 1000 s), which was the same for all three proteins, was subtracted (main plot) to facilitate the analysis of the exponential decay processes. The resultant fitted curves overlie the corrected data in the main plot.

congruent loss of transport efficiency, whereas R316A and F329A were more detrimental (about 10-fold) to  $K_m$  than to  $K_d$ . As in the binding determinations, double mutagenesis showed the impact of Y272 on transport: its

combinations with Y260A, F329A and R316A further decreased the overall uptake affinity, even though the transport properties of FepA were not impaired by Y272A alone.

#### Alanine substitutions for acidic residues

The triple-negative charge of FeEnt makes it unlikely that negatively charged residues directly participate in its recognition and binding. Nevertheless, the possibility of a complex network of electrostatic interactions in the binding site led us to evaluate the importance of acidic amino acids in the same region of FepA primary structure, using the same regimen of single and double Ala substitutions. Five acidic residues occur in the region bounded by residues 255 and 355, which localize to either the external vestibule (E280, E310, E319 and E326) or the periplasmic rim of the  $\beta$ -barrel (D298). Analysis of the 15 single and double combinations that we engineered for these acidic amino acids showed that only one created functional defects: E319A was deficient in both FeEnt binding and transport (Figs 3 and 6; Table 1), with  $K_d = 0.6$  nM and  $K_m = 9$  nM. Within error, all the other acidic substitution mutants functioned as well as FepA.

#### Effects of mutagenesis on colicin killing

Colicin B and D killed bacteria expressing the single and double mutants at, or very near, wild-type levels (Table 1), suggesting that unlike the conserved basic residues R286 and R316 the conserved aromatic residues that we studied are not essential to colicin penetration. For the aromatic replacement mutants, the

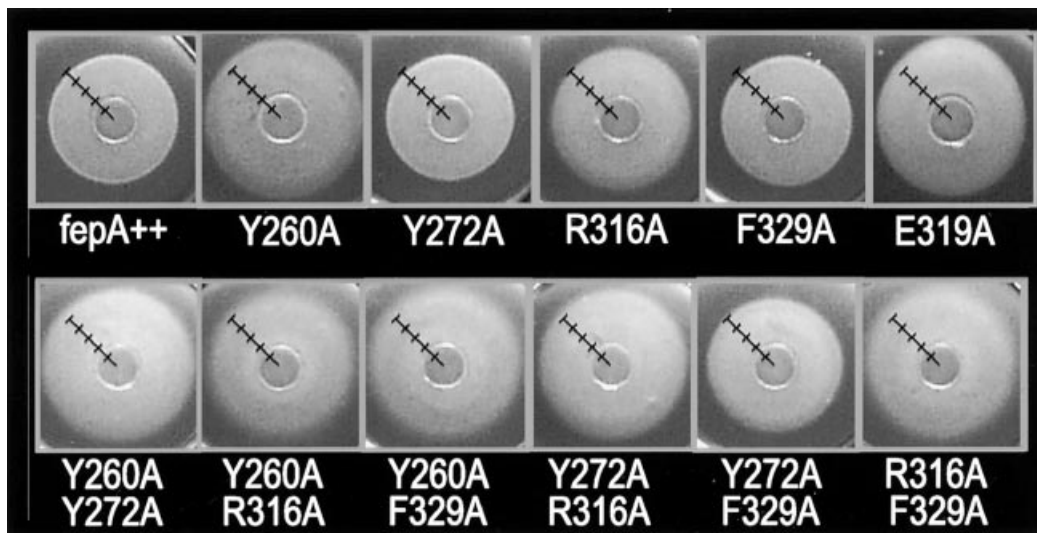


**Fig. 6.** Siderophore nutrition tests of FepA mutants. The photographs show *E. coli* strain KDF541 (*fepA*) containing plasmids expressing wild-type FepA or the indicated site-directed mutations after incubation at 37°C for 6–24 h. A 10 mm ruler is embedded in the photos.

**Table 2.** Kinetic constants of FeEnt association with mutant FepA proteins.

Protein <sup>a</sup>	$k_1^b$	$A_1^c$	$k_3$	$A_2$
E280C	0.68 ± 0.03	0.30 ± 0.005	0.30 ± 0.00001	0.24 ± 0.0006
E280C–Y272A–F329A	0.87 ± 0.06	0.26 ± 0.004	0.008 ± 0.0001	0.12 ± 0.001
E280C–Y260A–R316A	0.97 ± 0.07	0.33 ± 0.008	0.04 ± 0.002	0.09 ± 0.004

a. The proteins were purified, labelled with IAF, suspended in buffer at 25 nM, FeEnt was added to 10 μM, and the rates of association were measured by fluorescence spectroscopy.

b. Association rate constants, which were calculated based on a double exponential decay process, using GRAFIT 4, are denoted as described previously (Payne *et al.*, 1997).

c. The amplitudes of the exponential decays are expressed as relative values that were derived from the decrease in F/F<sub>0</sub>.

greatest effect was a twofold reduction in sensitivity. In contrast, R286A/R316A decreased colicin sensitivity 50- to 500-fold (Newton *et al.*, 1997). Even when they were combined with R316A, the most detrimental Ala-for-aromatic substitutions, Y260 and F329, did not further reduce susceptibility to colicins B and D (Table 1).

## Discussion

Any experimental study involving mutagenesis as a diagnostic tool of protein function must consider potential changes in global conformation as a possible artifact. Three independent lines of evidence argue against the idea that the reduced siderophore binding and transport abilities of the mutant proteins arose from unanticipated but debilitating conformational changes as a result of mutagenesis. All the single mutants produced relatively small decreases in affinity, which, when combined, were additive. All the mutants, including double mutants that were severely impaired in binding and transport of FeEnt, showed virtually wild-type levels of colicin susceptibility, indicating that both the surface structures and the general functionality of the mutant proteins remained intact. Finally, the overall results from the series of residues that we considered in the experiments, 13 aromatic, acidic and basic amino acids in surface loops, β-strands and on the rim of the β-barrel, in the same general region of FepA, pertain to the question of structural distortions from mutagenesis. With the exception of Y260, Y272, F329 and E319, which all reside in appropriate locations for contact with the siderophore, no deficiencies were found in any of the other mutant proteins. These data rebut the idea that the site-directed mutations caused significant conformational changes in the region of interest.

Eleven surface loops encircle the membrane channels of FepA and FhuA, forming a large external vestibule through which ferric siderophores enter. The individual loops of FepA are not homologous or even similar to those of FhuA: they differ in composition and in length (Ferguson *et al.*, 1998; Locher *et al.*, 1998; Buchanan *et al.*, 1999). In both proteins, however, aromatic amino acids that exist in different positions in different loops of the two OM proteins surround the vestibule mouth

(Fig. 1). The first conclusion of our experiments is that these exteriormost residues, which are predominantly tyrosines, create an initial binding site (called here B1) for ferric siderophores. The effects of Ala substitution at Y272, one of the residues that form the aromatic 'lips' of the vestibule, indicate that changes in B1 impair the binding and, consequently, also the transport of FeEnt. The more dramatic effects of substitution for F329 show that it plays a more important role in the initial recognition site. Furthermore, although the position of this residue was not observed in the crystal structure because of its high flexibility, the discovery of F329 in the epitope of an antibody that competitively inhibits FeEnt binding localizes the residue in a ligand recognition site, exactly as suggested by the mutagenesis results. Thus, the data support both the existence of the outer B1 site, which primarily functions by hydrophobic bonds, and the importance of aromatic residues F329 and Y272 within it. Although the catecholate nature of FeEnt led us to postulate the involvement of aromatic amino acids in its recognition by FepA, in fact, other OM proteins (FhuA, LamB) that interact with non-aromatic ligands also contain aromatic residues in their binding pockets, illustrating the generality of this adsorption mechanism.

Deeper within the vestibule mouth, FepA and FhuA diverge. The former protein, which transports a triple-anionic catecholate siderophore, contains an abundance of basic residues grouped in a cluster at the top of its N-terminal domain. The latter protein, which transports an uncharged, hydrophobic, hydroxamate peptide siderophore, contains a concentration of aromatic residues in the same relative position. The properties of these potential secondary sites (B2) match the chemical attributes of the compounds that they recognize, perhaps conferring specificity to the binding reaction. The FhuA crystal structures contained ferrichrome bound in the B2 region. Although the FepA crystal structure did not resolve the position of FeEnt in the loops (it showed partial occupancy in their outer extremities; Buchanan *et al.*, 1999), the co-ordinates depict R316 and Y260 within B2, appropriately located to interact with the ferric siderophore as it approaches and transits the channel (Fig. 1). The functional importance of Y260 constitutes a second conclusion of



our experiments: the 100-fold reduction in affinity from Y260A is the largest effect of a single mutation seen in FepA so far, suggesting that the high affinity for FeEnt derives from interactions within the B2 site. The 2500-fold reduction in binding and transport seen in the Y260A/R316A double mutant leaves no doubt about the importance of B2 in siderophore acquisition. This region contains charged and aromatic amino acids, suggesting that both hydrophobic and electrostatic bonds contribute to its functionality. The proximity of the E319 carboxylate moiety (7 Å from the guanidino group of R316) underscores the inference of ionic interactions within the B2 site.

The hypothesis of two FeEnt binding sites in FepA originated from *in vitro* fluorescence measurements that showed kinetically discernible stages of FeEnt adsorption (Payne *et al.*, 1997), and our rate measurements of binding by site-directed mutants corroborate and extend this theory. The adsorption of FeEnt quenches the emission spectrum of fluoresceinated FepA by about 60%, and the drop in fluorescence is consistent with the sum of two sequential exponential decay processes. The high-affinity, saturation effects of FeEnt on the fluorescent reporter group (Payne *et al.*, 1997) imply that the quenching does not originate from direct, non-specific collisions between the siderophore and fluorescein; the distance of E280C from the mouth of the FepA vestibule (Fig. 1; Buchanan *et al.*, 1999) strengthens this conclusion. Thus, the time-dependent decrease in fluorescence intensity derives from a permutation of FepA structure that changes the environment of the fluorescent label. In the mutants, the magnitude of quenching by FeEnt was less than in wild-type FepA, indicating that they underwent different conformational changes. Double mutagenesis of Y260 and R316 increased the amplitude of the first stage, and virtually eliminated the second stage. A straightforward interpretation of these results is that FeEnt binding causes one conformational change when it associates with the outer site, and another change when it moves to the inner site. In view of this, the Y260A/R316A mutation seriously compromised the second site, without measurable effects on the first and, as a result, the first binding phase predominated. This explanation also rationalizes the tendency of Y260A to retard progress towards binding equilibrium. Ala substitution for Y272 and F329, on the other hand, affected both stages of the association reaction. This result is consistent with the idea that decreased efficiency of the initial binding will also reduce the extent of ligand movement to the second site. Consequently, the amplitudes of both stages will lessen. It is noteworthy that more complex, alternative explanations are also plausible. Presteady-state experiments are needed to clarify the respective roles of B1 and B2 in the overall uptake process. In spite of this caveat, the

spectroscopic results verify the existence of the B1 and B2 sites, which are kinetically, conformationally and functionally linked in the FeEnt association reaction. Thus, another conclusion of the experiments is that the first binding stage abstracts the ligand from solution into B1, whereas the second step involves inward movement of FeEnt to B2, where it sits poised above the transmembrane channel before transport.

The characteristic catechol groups of ferric enterobactin provide several potential modes of interaction between FeEnt and FepA. Aromatic rings may act as hydrogen bond acceptors (Levitt and Perutz, 1988; Mitchell *et al.*, 1994), and they may form planar stacking interactions with other ring systems and with arginines (Flocco and Mowbray, 1994). Van der Waals' forces and hydrophobic effects may also determine ligand interaction behaviour with proteins (Kuntz *et al.*, 1999). In low-affinity protein recognition systems, hydrophobic interactions often provide affinity for ligand adsorption, whereas charge-charge interactions are responsible for recognition specificity (Davis *et al.*, 1998). In this case, electrostatic forces usually contribute by creating a correct conformation or alignment that leads to complementarity between the ligand and its receptor (Jones and Thornton, 1996). On the other hand, in high-affinity recognition systems, charge-charge interactions may provide not only elements of specificity, but also enhanced ligand affinity (Chong *et al.*, 1999). Our experiments suggest that the FeEnt-FepA binding equilibrium exhibits both kinds of interactions: the B1 site functions by hydrophobic bonds, whereas in B2, hydrophobic and electrostatic forces combine to create an extremely precise (Thulasiraman *et al.*, 1998), avid (Newton *et al.*, 1999) recognition phenomenon. The adsorption reaction is sensitive to alterations in these chemical characteristics of FepA, and double mutagenesis confirmed the multideterminant nature of the interaction: when two apparent contact residues were removed from FepA, whether two aromatic, two basic, or one of each, a substantial decrease in the receptor function (> 1000-fold) occurred.

The independence of colicin killing from the aromatic residues that are important in FeEnt utilization was unexpected. F329 and Y272, which exist in the peripheral interface between the protein and the aqueous environment, were dispensable to colicin penetration. Furthermore, two positively charged amino acids in the interior of FepA, R286 and R316, were essential to colicin B and D susceptibility, but Y260, which was required for optimal FeEnt binding and transport, was also dispensable to colicin penetration. The close proximity of Y260 to R316 suggests that the positive charge of the latter amino acid, rather than its location, is most relevant to colicin reception.

The experiments described here and other studies

(Rutz *et al.*, 1992; Newton *et al.*, 1997) used mutagenesis to investigate the relationship between structure and function in FepA. An initial perception of the research, upon which some of our mutagenesis targets were based, was that one or a few surface loops in the central part of FepA sequence (L3, L4, L5) are pre-eminent in the recognition and binding of FeEnt. The primary argument against this conclusion is that FepA functions, albeit at much reduced efficiency, without these single loops (Newton *et al.*, 1999). The current experiments provide insight into this result. The OM protein contains two binding sites for the ferric siderophore, one formed by residues in the loop extremities, and the other deep in the vestibule, primarily composed of side-chains from the interior barrel wall, and perhaps also residues in the N-terminal domain (although our data do not address this region). Single loop deletions did not abrogate FeEnt recognition and binding because (i) multiple loops participate in the initial adsorption reaction (evidenced by the identification of Y272 in L3 and F329 in L4); and (ii) they did not eliminate the secondary, underlying binding site (involving at least Y260 and R316). It is likely that other loops contribute contact residues to the binding reaction (Fig. 1), so we are left with the perception of two multideterminant binding domains formed by the coalescence of residues distributed throughout FepA primary structure. As the precision of the mutagenic approach escalated, it revealed this final conclusion with increasing certainty.

## Experimental procedures

### Bacterial strains and media

*Escherichia coli* K-12 strains were grown in Luria–Bertani broth (Miller, 1972), Tris media (Klebbba *et al.*, 1982) or MOPS media (Neidhardt *et al.*, 1974).

### Sequence comparisons

The sequences of six FeEnt transporters from *E. coli* (Lundrigan and Kadner, 1986), *Salmonella typhimurium* (Tumumuru *et al.*, 1990), *Pseudomonas aeruginosa* (Dean and Poole, 1993), *Salmonella enterica* (Baumler *et al.*, 1998), *Bordetella pertussis* (Beall and Sanden, 1995) and five other *E. coli* LGPs, FecA, BtuB, IutA, FhuA and FhuE were compared using the PILEUP program (Genetics Computer Group, Madison, WI, USA). The alignment was manually adjusted on the basis of the *E. coli* FepA crystal structure (Buchanan *et al.*, 1999).

### Site-directed mutagenesis

We previously used pITS449 (Armstrong *et al.*, 1990) as the starting point for site-directed mutagenesis. In the present work, we created vector pT944, a pITS449 derivative that incorporates restriction sites without changing the *fepA* coding sequence. pT944 introduced a *Sma*I site at position

126 (GCCCCGCGAT to GCCCCGGGAT), removed the methylation site for *Cl*I at position 1023 (ATCGATCTT to ATCGATTTA) and introduced a *Bam*HI site at position 1701 (GGATCG to GGATCC). These modifications facilitate manipulation of the vector when combining independent mutations. Using *Pst*I and *Sac*I sites, the *fepA* structural gene from pT944 was inserted into the multiple cloning site of M13 mp19. To create individual *fepA* mutants, we performed site-directed mutagenesis with the structural gene in M13 (Kunkel, 1985). The mutation in *fepA* was then cloned back into the pT944 *fepA* structural gene using appropriate restriction sites and enzymes. The entire mutant gene was sequenced to rule out any random mutagenesis. The resultant plasmids were finally transformed into KDF541 (*fepA*; Rutz *et al.*, 1992).

### Expression

KDF541 strains harbouring pITS449, pT944 or their mutant derivatives were grown in LB broth with ampicillin and streptomycin (both at 100  $\mu\text{g ml}^{-1}$ ) for 16 h at 37°C before subculture at 1% into MOPS media with ampicillin (10  $\mu\text{g ml}^{-1}$ ). After growth for 5.5 h at 37°C with vigorous aeration,  $5 \times 10^7$  bacteria cells were collected by centrifugation and lysed by boiling with SDS–PAGE sample buffer. After electrophoresis on 10% slabs, the separated proteins were transferred to nitrocellulose paper, which was analysed by immunoblotting with anti-FepA mAb 41 or mAb 45 and [<sup>125</sup>I]-protein A (Newton *et al.*, 1997).

### FeEnt binding

We intended to use alanine scanning mutagenesis, in conjunction with thermodynamic and kinetic analyses, to elucidate the FeEnt–FepA interaction, but the necessity of double substitutions expanded the scope of the experiments so much that screening methods were required to find constructs of interest for further study. Affinity screening was the improvement that expedited the experiments. The finding that prior binding and transport methodologies underestimated the affinities of ferric siderophore–receptor systems as much as 50 000-fold (Newton *et al.*, 1999) focused our attention in the subnanomolar range, and the ratio of wild-type  $K_d$  or  $K_m$  ( $\approx 0.1$  nM) to a second, much higher concentration readily identified mutants with defects. The methodological corrections also facilitated accurate characterization of both single and double mutants. It did not, however, alleviate the need for double mutagenesis: Y272A again illustrated the concept that substitution for a functionally relevant residue may not compromise a multivalent ligand–receptor interaction (Newton *et al.*, 1997).

To quickly assess siderophore binding, we compared <sup>59</sup>FeEnt adsorption (Newton *et al.*, 1999) at the wild-type  $K_d$  and a much higher concentration. Mutants that were impaired in the binding screen were further analysed by determination of their  $K_d$  and capacity for <sup>59</sup>FeEnt (Newton *et al.*, 1999). For FepA and mildly defective mutants,  $2 \times 10^7$  cells were tested with <sup>59</sup>FeEnt at approximately 200 c.p.m.  $\text{pmol}^{-1}$ ; for more impaired mutants, 10 times more cells were assayed, and the <sup>59</sup>FeEnt was diluted with non-radioactive FeEnt to reduce the

specific activity to about 20 c.p.m.  $\text{pmol}^{-1}$ . For even more severely defective constructs,  $5 \times 10^8$  cells were used, and  $^{59}\text{FeEnt}$  was prepared at about 10 c.p.m.  $\text{pmol}^{-1}$ . Both screening assays and  $K_d$  determinations were corrected with measurement of  $^{59}\text{FeEnt}$  binding to the negative control KDF541; the data were analysed by GRAFIT 4.

#### FeEnt uptake

To quickly assess siderophore transport, we performed siderophore nutrition tests (Newton *et al.*, 1999) and compared  $^{59}\text{FeEnt}$  uptake (Newton *et al.*, 1999) by screening at the wild-type  $K_m$  and a much higher concentration. Mutants of interest were further characterized by determination of transport  $K_m$  and  $V_{\text{max}}$ . As with the binding experiments, uptake assays on mutants with decreased capabilities required an increase in the number of cells and a decrease in the specific activity of  $^{59}\text{FeEnt}$ . In addition, the incubation times of the transport experiments were increased (from 15 s for wild-type FepA to up to 2 min) to accommodate the lower uptake rates of the mutants. GRAFIT 4 was used to determine the thermodynamic and kinetic parameters.

#### Fluorescence measurements

Purified FepA proteins containing the E280C mutation (final concentration 0.15 mg  $\text{ml}^{-1}$ ) in TTE buffer (50 mM Tris, pH 7.2, 2% Triton X-100, 5 mM EDTA) were incubated with 10  $\mu\text{M}$  5-iodoacetamidofluorescein (IAF; Molecular Probes) at room temperature in the dark with shaking for 45 min, ethanol precipitated three times and resuspended in 1 mM n-dodecyl  $\beta$ -D-maltoside (DM; Sigma), 50 mM MOPS, pH 7.0, 60 mM NaCl buffer. The reaction was then transferred to dialysis tubing (MWCO 12 000–14 000) and dialysed against the above buffer at 4°C with three changes of buffer for 48 h to remove unreacted probes. The concentration of the labelled proteins was determined before storage at  $-80^\circ\text{C}$ .

In the FeEnt binding time course measurement, E280C labelled with IAF was diluted into 1 mM DM, 50 mM MOPS, pH 7.0, 60 mM NaCl buffer to a final concentration of 25 nM and incubated at 25°C for 1 h to ensure the stabilization of E280C–IAF. The time course was then started on the SLM8100 fluorimeter at an excitation and an emission wavelength of 490 nm and 520 nm, respectively, with the slits all set at 4 nm and an integration time of 1 s. After about 5 min of prerun, ferric enterobactin in 50 mM MOPS, pH 7.0, 60 mM NaCl was added to a final concentration of 10  $\mu\text{M}$ . The same fluorescent labelling and time course measurement procedures were performed on Y272A–F329A–E280C and Y260A–R316A–E280C mutants. Wild-type protein FepA was used as a control.

#### Colicin killing

To examine the colicin sensitivity of each mutant FepA, a series of twofold dilution of colicins B and D were made in LB broth in a 96-well microplate. Using a Clonemaster (Immusine), 5  $\mu\text{l}$  of diluted ColB or ColD was then transferred from the master plate to LB agar plated with KDF541 harbouring pITS449 or its mutant derivatives. After incubation at 37°C overnight, sensitivity was expressed as the maximum

colicin dilution that resulted in clearing of the bacterial lawn to the agar.

#### Acknowledgements

We thank Marjorie A. Montague for expert technical assistance, and Dick van der Helm, Marvin A. Payne and Paul F. Cook for critical reading of the manuscript. This study was supported by grants from the National Science Foundation (MCB9709418) and the National Institutes of Health (GM53836) to P.E.K., and OCAST grant 000072 to S.M.C.N. Dr Cook's contributions were supported by the Grayce B. Kerr Centennial Professorship in Biochemistry.

#### References

- Armstrong, S.K., Francis, C.L., and McIntosh, M.A. (1990) Molecular analysis of the *Escherichia coli* ferric enterobactin receptor FepA. *J Biol Chem* **265**: 14536–14543.
- Baumler, A.J., Norris, T.L., Lasco, T., Voight, W., Reissbrodt, R., Rabsch, W., *et al.* (1998) IroN, a novel outer membrane siderophore receptor characteristic of *Salmonella enterica*. *J Bacteriol* **180**: 1446–1453.
- Beall, B., and Sanden, G.N. (1995) A *Bordetella pertussis* fepA homologue required for utilization of exogenous ferric enterobactin. *Microbiology* **141**: 3193–3205.
- Buchanan, S.K., Smith, B.S., Venkatramani, L., Xia, D., Esser, L., Palnitkar, M., *et al.* (1999) Crystal structure of the outer membrane active transporter FepA from *Escherichia coli*. *Nature Struct Biol* **6**: 56–63.
- Cao, Z. (1999) PhD Thesis. University of Oklahoma.
- Chong, L.T., Duan, Y., Wang, L., Massova, I., and Kollman, P.A. (1999) Molecular dynamics and free-energy calculations applied to affinity maturation in antibody 48G7. *Proc Natl Acad Sci USA* **96**: 14330–14335.
- Davis, S.J., Davies, E.A., Tucknott, M.G., Jones, E.Y., and van der Merwe, P.A. (1998) The role of charged residues mediating low affinity protein–protein recognition at the cell surface by CD2. *Proc Natl Acad Sci USA* **95**: 5490–5494.
- Dean, C.R., and Poole, K. (1993) Cloning and characterization of the ferric enterobactin receptor gene (*pfeA*) of *Pseudomonas aeruginosa*. *J Bacteriol* **175**: 317–324.
- Ferguson, A.D., Hofmann, E., Coulton, J.W., Diederichs, K., and Welte, W. (1998) Siderophore-mediated iron transport: crystal structure of FhuA with bound lipopolysaccharide. *Science* **282**: 2215–2220.
- Flocco, M.M., and Mowbray, S.L. (1994) Planar stacking interactions of arginine and aromatic side-chains in proteins. *J Mol Biol* **235**: 709–717.
- Jiang, X., Payne, M.A., Cao, Z., Foster, S.B., Feix, J.B., Newton, S.M., *et al.* (1997) Ligand-specific opening of a gated-porin channel in the outer membrane of living bacteria. *Science* **276**: 1261–1264.
- Jones, S., and Thornton, J.M. (1996) Principles of protein–protein interactions. *Proc Natl Acad Sci USA* **93**: 13–20.
- Killmann, H., Benz, R., and Braun, V. (1993) Conversion of the FhuA transport protein into a diffusion channel through the outer membrane of *Escherichia coli*. *EMBO J* **12**: 3007–3016.
- Klebba, P.E., McIntosh, M.A., and Neilands, J.B. (1982)

- Kinetics of biosynthesis of iron-regulated membrane proteins in *Escherichia coli*. *J Bacteriol* **149**: 880–888.
- Kuhn, S.E., Nardin, A., Klebba, P.E., and Taylor, R.P. (1998) *Escherichia coli* bound to the primate erythrocyte complement receptor via bispecific monoclonal antibodies are transferred to and phagocytosed by human monocytes in an *in vitro* model. *J Immunol* **160**: 5088–5097.
- Kunkel, T.A. (1985) Rapid and efficient site-specific mutagenesis without phenotypic selection. *Proc Natl Acad Sci USA* **82**: 488–492.
- Kuntz, I.D., Chen, K., Sharp, K.A., and Kollman, P.A. (1999) The maximal affinity of ligands. *Proc Natl Acad Sci USA* **96**: 9997–10002.
- Levitt, M., and Perutz, M.F. (1988) Aromatic rings act as hydrogen bond acceptors. *J Mol Biol* **201**: 751–754.
- Liu, J., Rutz, J.M., Feix, J.B., and Klebba, P.E. (1993) Permeability properties of a large gated channel within the ferric enterobactin receptor, FepA. *Proc Natl Acad Sci USA* **90**: 10653–10657.
- Locher, K.P., Rees, B., Koebnik, R., Mitschler, A., Moulinier, L., Rosenbusch, J.P., *et al.* (1998) Transmembrane signaling across the ligand-gated FhuA receptor: crystal structures of free and ferrichrome-bound states reveal allosteric changes. *Cell* **95**: 771–778.
- Lundrigan, M.D., and Kadner, R.J. (1986) Nucleotide sequence of the gene for the ferrienterochelin receptor FepA in *Escherichia coli*: Homology among outer membrane receptors that interact with TonB. *J Biol Chem* **261**: 10797–10801.
- Miller, J.H. (1972) *Experiments in Molecular Genetics*. Cold Spring Harbor, NY: Cold Spring Harbor Laboratory Press.
- Mitchell, J.B., Nandi, C.L., McDonald, I.K., Thornton, J.M., and Price, S.L. (1994) Amino/aromatic interactions in proteins: is the evidence stacked against hydrogen bonding? *J Mol Biol* **239**: 315–331.
- Murphy, C.K., Kalve, V.I., and Klebba, P.E. (1990) Surface topology of the *Escherichia coli* K-12 ferric enterobactin receptor. *J Bacteriol* **172**: 2736–2746.
- Neidhardt, F.C., Bloch, P.L., and Smith, D.F. (1974) Culture medium for enterobacteria. *J Bacteriol* **119**: 736–747.
- Newton, S.M., Allen, J.S., Cao, Z., Qi, Z., Jiang, X., Sprencel, C., *et al.* (1997) Double mutagenesis of a positive charge cluster in the ligand-binding site of the ferric enterobactin receptor, FepA. *Proc Natl Acad Sci USA* **94**: 4560–4565.
- Newton, S.M., Igo, J.D., Scott, D.C., and Klebba, P.E. (1999) Effect of loop deletions on the binding and transport of ferric enterobactin by FepA. *Mol Microbiol* **32**: 1153–1165.
- Payne, M.A., Igo, J.D., Cao, Z., Foster, S.B., Newton, S.M., and Klebba, P.E. (1997) Biphasic binding kinetics between FepA and its ligands. *J Biol Chem* **272**: 21950–21955.
- Rutz, J.M., Liu, J., Lyons, J.A., Goranson, J., Armstrong, S.K., McIntosh, M.A., *et al.* (1992) Formation of a gated channel by a ligand-specific transport protein in the bacterial outer membrane. *Science* **258**: 471–475.
- Thulasiraman, P., Newton, S.M., Xu, J., Raymond, K.N., Mai, C., Hall, A., *et al.* (1998) Selectivity of ferric enterobactin binding and cooperativity of transport in gram-negative bacteria. *J Bacteriol* **180**: 6689–6696.
- Tumumuru, M.K.R., Armstrong, S.K., and McIntosh, M.A. (1990) In *American Society for Microbiology Annual Meeting*. Atlanta, GA: American Society of Microbiology Press. p. 69.